Journal of Sound and Vibration (1997) **206**(3), 339–352

SPLINE FINITE MEMBER ELEMENT METHOD FOR VIBRATION OF THIN-WALLED MEMBERS WITH SHEAR LAG

Q.-F. WANG

Dept. of Civil Engineering, *National Huaqiao University*, *Quanzhou* 362011, *Fujian*, *People's Republic of China*

(*Received* 26 *January* 1996, *and in final form* 11 *April* 1997)

In this paper, the outlined model is extended to cover the dynamics of thin-walled members with open or closed cross-section, making use of Hamilton's principle. Based on the displacement variational principle, a systematic method, called the spline finite member element method, is developed for vibration analysis of thin-walled members with arbitrary cross-section. The displacements at two ends of the member element are adopted as basic variables in the method. A transformed B_3-spline function is used to simulate the warping displacements along the cross-section of the thin-walled member. The analysis takes into account the effect of shearing strains of the middle surface of walls on the vibration, which reflect the shear lag phenomenon. To verify the accuracy and efficient of the proposed method, four experiments are conducted in which the present results are compared with those using other analytical methods and the "COSMOS/M" finite element analysis program.

1. INTRODUCTION

Many structures, such as a shear wall core or a frame-shear wall structure, are typically idealized as thin-walled members that exhibit significant out-of-plane warping due to torsion. Urgent practical requirements have given rise in recent years to extensive investigations, both theoretical and experimental, of the dynamic analysis of the thin-walled structural members. Some closed form solutions for small amplitude vibrations of such members were published by Vlasov [1]. Useful explicit formulae to determine the lowest natural flexural and torsional frequencies for thin-walled members with open and/or closed cross-section can also be found in other publications [2–4]. However, these methods cannot evince the shear lag effect in their results. When the structure exhibits a considerable flexural stiffness, as in the shear wall core of a building, shear strains play an important role even in the presence of lower frequencies. The shear lag phenomenon was first recognized by Timoshenko, who introduced two distinct functions, i.e., the deflection of the centroid of the cross-section and the rotation of the normal to the cross-section through the centroid [5]. In Timoshenko's theory the warping of the cross-section, proportional to the shear resultant, can vary along the member axis without giving rise to additional stresses (shear lag). By giving an alternative definition of the two unknown functions introduced by Timoshenko, Cowper proposed a more appropriate way of determining the shear coefficient [6, 7]. However, these solutions were often restricted to particular cross-section shapes and are generally difficult to apply. Friberg [8] solved Vlasov's equations [1] analytically and formed the exact dynamic stiffness matrix without the assumption of cross-sectional symmetry of the member. Among the previous methods for

0022–460X/97/380339 + 14 $25.00/0/sv971097

dynamic analysis, the finite element method is widely used for vibration and buckling analyses of structures, including thin-walled structures [9, 10]. However, to obtain an accurate solution in the analysis, a large number of elements are required, resulting in a heavy consumption of CPU time and data preparation and manipulation efforts. Therefore, its application to practical design for a complex thin-walled structure is greatly limited. On the other hand, some deficiencies in the classical theory [1] have yet to be solved or improved. For instance, in the theory there are two different approaches for analyzing thin-walled members with an open cross-section and those with a closed cross-section; i.e., Vlasov's theory for the former and Umansky's theory for the latter. In engineering practice, a lot of thin-walled members have mixed cross-sections composed of pure open walls and closed cells. Therefore, it is of practical significance to develop a general consistent method for dynamic analysis of thin-walled members with any cross-section. Four typical numerical examples are used to demonstrate the versatility, accuracy and convergency of the proposed method. It can be observed clearly in the results that the present method may be a type of systematic method which can be applied to the dynamic analysis of thin-walled members of any cross-section with branches of walls, and which can save much more computing time than the standard finite element analysis program.

In this paper, only one of two Vlasov' assumptions, i.e. the "rigid cross-section" is retained, while the condition of no shearing strain in the middle surface of walls is abandoned. Also, another common assumption is adopted, i.e., the stress σ_s in the tangent direction and the stress σ_n in the normal direction of the central line of the cross-section are much smaller than the longitudinal stress σ_z and both are neglected in the dynamic analysis.

2. ENERGY EQUATION OF THIN-WALLED MEMBER

A member element of a prismatic thin-walled member with arbitrary cross-section is shown in Figure 1, in which the z-axis is the longitudinal axis, the x- and y-axes are the principal axes passing through the centroid c of the cross-section; s is the curvilinear co-ordinate along the central line of the cross-section; and H is the longitudinal length of the member element.

The Hamilton principle in variation form for free vibration can be expressed as follows:

$$\delta \int_{t_1}^{t_2} (T - U)\, \mathrm{d}t = 0, \tag{1}$$

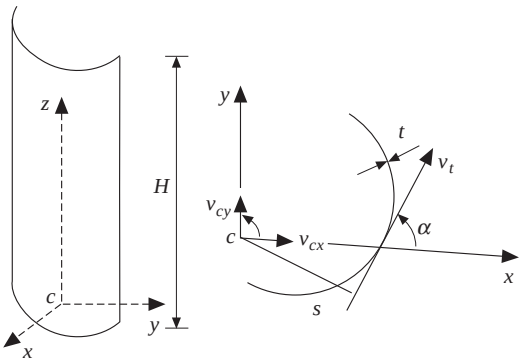

Figure 1. An arbitrary cross-section of a thin-walled member and its parameters.

in which U is the possible strain energy induced in vibration; T is the corresponding possible kinetic energy. The integral interval can be chosen as

$$t_1 = 0, \qquad t_2 = 2\pi/\omega,$$

in which ω is the circular frequency of vibration.

The possible strain energy [11] and the possible kinetic energy in a general member element of length H can be given by the expression

$$U = \tfrac{1}{2}\int_0^H \left\{ \int_{\Sigma s} \left[E\left(\frac{\partial w}{\partial z}\right)^2 t_0 + G\left(\frac{\partial w}{\partial s} + \frac{\partial v_t}{\partial z}\right)^2 t \right] \mathrm{d}s + GJ_d\left(\frac{\mathrm{d}\theta}{\mathrm{d}z}\right)^2 \right\} \mathrm{d}z; \tag{2}$$

$$T = \tfrac{1}{2}\int_0^H \int_{\Sigma s} \rho_0 \left[\left(\frac{\partial w}{\partial t}\right)^2 t_0 + \left(\frac{\partial v_x}{\partial t}\right)^2 t + \left(\frac{\partial v_y}{\partial t}\right)^2 t \right] \mathrm{d}s\, \mathrm{d}z, \tag{3}$$

in which $w(s, z)$ is the longitudinal displacement along the z direction; v_t is the displacement along the tangent direction of the central line at point s; θ is the twisting angle of the cross-section; v_x and v_y are the displacements of any point of the cross-section in the x and y directions respectively; E is Young's modulus; G is the shear modulus; J_d is the St. Venant's torsional constant; ρ_0 is the density of material of the member; Σs is the length of the whole cross-section; t_0 is the actual thickness of the wall at point s; and t is the equivalent thickness of the wall when there is a row of holes in the wall.

According to the "rigid cross-section" assumption [1], the tangent displacement can be expressed by the centroid displacement

$$v_t(z) = v_{cx}\cos\alpha + v_{cy}\sin\alpha + \rho\theta,$$

in which α is the angle between the x-axis and the tangent of point s; $\rho(s)$ is the distance from c to the tangent of point s; and v_{cx} and v_{cy} are the x and y direction components of the centroid displacement v_c respectively. It can be written in matrix form

$$v_t(z) = [\eta_t]_{1\times 3}\{v_c\}_{3\times 1}, \tag{4}$$

in which

$$[\eta_t] = [\cos\alpha \quad \sin\alpha \quad \rho],$$
$$\{v_c\} = [v_{cx} \quad v_{cy} \quad \theta]^{\mathrm{T}}. \tag{5}$$

3. LONGITUDINAL WARPING DISPLACEMENT FUNCTION

The ordinary cubic B_3-spline function, because of its localized nature, not only reduces computational effort, but also allows different boundary conditions to be specified by slightly modifying a few local spline functions. Owing to the complexity of the cross-section of thin-walled members, especially for the cross-section with branches of walls, it is difficult to use the ordinary B_3-spline function properly to simulate the longitudinal displacement at the bifurcate point of the walls. Therefore, a new modified B_3-spline function is needed to overcome this defect. By the separation of variables and semi-discrete technique, the longitudinal warping displacement $w(s, z)$ is taken as the summation of $(m + 3)$ local B_3-splines by

$$w(s, z) = \sum_{i=1}^{m+3} \alpha_i(z)\psi_i(s), \tag{6}$$

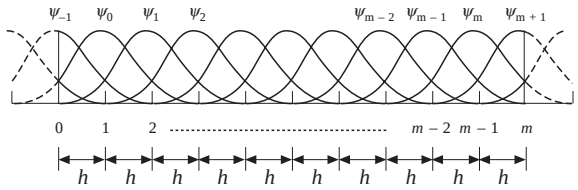

Figure 2. The sub-intervals of a segment.

in which α_i is the node generalized displacement parameters; m is the number of equal sub-intervals of a segment of the cross-section as shown in Figure 2, and ψ_i is an ordinary local B_3-spline as shown in Figure 3, defined by

$$\psi_i(s) = \frac{1}{6h^3}\begin{cases} (s - s_i + 2h)^3 & [s_{i-2}, s_{i-1}], \\ (s - s_i + 2h)^3 - 4(s - s_i + h)^3 & [s_{i-1}, s_i], \\ (s_i + 2h - s)^3 - 4(s_i + h - s)^3 & [s_i, s_{i+1}], \\ (s_i + 2h - s)^3 & [s_{i+1}, s_{i+2}], \end{cases} \tag{7}$$

in which s_i is the node co-ordinate; $h = s_{i+1} - s_i$, and h is its equal section length.

Let w_j be the real node displacement in the segment, i.e.,

$$\begin{aligned} w_1 &= \frac{\partial w(s_2, z)}{\partial s}, \\ w_2 &= w(s_2, z), \\ &\cdots \\ w_i &= w(s_i, z), \\ &\cdots \\ w_{m+2} &= w(s_{m+2}, z), \\ &\cdot \\ w_{m+3} &= \frac{\partial w(s_{m+2}, z)}{\partial s} \end{aligned} \tag{8}$$

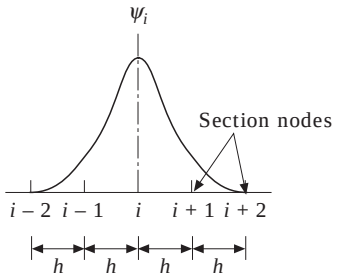

Figure 3. The ordinary local B_3-spline of equal section length.

in which s_2 and s_{m+2} are the co-ordinates of the beginning and the end nodes in the segment respectively. Because of the localization of the spline function, equation (6) can be expressed by m interval functions as

$$w_{sj}(s, z) = \sum_{i=j-2}^{j+1} \alpha_i(z)\psi_i(s), \qquad s_{j-1} \leqslant s \leqslant s_j, \quad j = 3, 4, 5, \ldots, m+2; \tag{9}$$

Combining equations (7), (8) and (9), we have

$$\begin{gathered} w_1 = \frac{1}{2h}(\alpha_3 - \alpha_1), \\ \cdots \\ w_i = \tfrac{1}{6}(\alpha_{i-1} + 4\alpha_i + \alpha_{i+1}), \qquad i = 2, 3, \ldots, m+2, \\ \cdots \\ w_{m+3} = \frac{1}{2h}(\alpha_{m+3} - \alpha_{m+1}); \end{gathered} \tag{10}$$

Solving the above simultaneous equations using the package "Maple V" [12], the node general displacement parameters α_i $(i = 1, 2, \ldots, m+3)$ can be expressed by real node displacements w_i as follows:

$$\alpha_i = \sum_{k=1}^{m+3} b_{ik} w_k, \qquad i = 1, 2, \ldots, m+3, \tag{11}$$

in which b_{ik} are the coefficients computed by means of the package "Maple V".

Substituting the above equation into equation (9) gives

$$\begin{aligned} w_{sj}(s, z) &= \sum_{k=1}^{m+3} \left[\sum_{i=j-2}^{j+1} b_{ik}\psi_i(s) \right] w_k(z) \\ &= \sum_{k=1}^{m+3} \bar{\psi}_{jk}(s) w_k(z), \qquad s_{j-1} \leqslant s \leqslant s_j, \quad j = 3, 4, \ldots, m+2, \end{aligned} \tag{12}$$

in which

$$\bar{\psi}_{jk}(s) = \sum_{i=j-2}^{j+1} b_{ik}\psi_i(s), \qquad s_{j-1} \leqslant s \leqslant s_j, \quad j = 3, 4, \ldots, m+2,$$

is called the "transformed spline function" and is constructed from four ordinary local B_3-spline functions $\psi(s)$. Because the parameters of the transformed spline function in every segment, including the four of the two ends, are the real node displacement parameters, this new simulation technique will overcome the difficulty of the ordinary spline function in simulating the cross-section with branches of walls. Finally, the longitudinal warping displacement $w(s, z)$ of the whole cross section can be expressed as

$$w(s, z) = \sum_{i=1}^{n} \bar{\psi}_i(s) w_i(z) = [\bar{\psi}]_{1 \times n} \{w\}_{n \times 1}, \tag{13}$$

in which n denotes the total number of nodes which divided the whole cross-section into sub-intervals, and

$$[\bar{\psi}]_{1\times n} = [\bar{\psi}_1(s), \bar{\psi}_2(s), \ldots, \bar{\psi}_n(s)],$$

$$\{w\}_{n\times 1} = [w_1(z), w_2(z), \ldots, w_n(z)]^{\mathrm{T}}.$$

4. DYNAMIC EQUATIONS OF THIN-WALLED MEMBER

As to free vibration at a natural frequency of the thin-walled member, the motion at any point is simple, harmonic, and the deflected shapes are independent of time. Equations (4) and (13) can be written as

$$v_t(z, t) = \bar{v}_t(z)\sin(\omega t + \varepsilon) = [\eta_t]_{1\times 3}\{\bar{v}_c\}_{3\times 1}\sin(\omega t + \varepsilon), \tag{14}$$

$$w(s, z, t) = \bar{w}(s, z)\sin(\omega t + \varepsilon) = [\bar{\psi}]_{1\times n}\{\bar{w}\}_{n\times 1}\sin(\omega t + \varepsilon), \tag{15}$$

in which $v_t(z)$ and $w(s, z)$ are the mode shape functions and ε is the phase angle.

Provided that the x- and y-axes are the principal axes passing through the centroid c of a cross-section, v_x and v_y are related to v_{cx}, v_{cy} and θ by

$$v_x(y, z, t) = (v_{cx} - y\theta)\sin(\omega t + \varepsilon),$$

$$v_y(x, z, t) = (v_{cy} + x\theta)\sin(\omega t + \varepsilon).$$

Substituting equations (14) and (15) into equations (2) and (3) gives

$$U = \tfrac{1}{2}\int_0^H (E\{w'\}^{\mathrm{T}}[A]\{w'\} + G\{w\}^{\mathrm{T}}[B]\{w\} + 2G\{w\}^{\mathrm{T}}[C]\{v_c'\} + G\{v_c'\}^{\mathrm{T}}[D_t]\{v_c'\} + G\{\theta'\}^{\mathrm{T}}J_d\{\theta'\})\,\mathrm{d}z, \tag{16}$$

$$T = \tfrac{1}{2}\int_0^H \rho_0\omega^2(\{w\}^{\mathrm{T}}[A]\{w\} + \{v_c\}^{\mathrm{T}}[\bar{D}]\{v_c\})\,\mathrm{d}z, \tag{17}$$

in which the superscript prime represents $\mathrm{d}()/\mathrm{d}z$; and

$$[A]_{n\times n} = \int_{\Sigma s}[\bar{\psi}]^{\mathrm{T}}[\bar{\psi}]t\,\mathrm{d}s, \qquad [B]_{n\times n} = \int_{\Sigma s}[\bar{\psi}']^{\mathrm{T}}[\bar{\psi}']t\,\mathrm{d}s,$$

$$[C]_{n\times 3} = \int_{\Sigma s}[\bar{\psi}']^{\mathrm{T}}[\eta_t]t\,\mathrm{d}s, \qquad [D_t]_{3\times 3} = \int_{\Sigma s}[\eta_t]^{\mathrm{T}}[\eta_t]t\,\mathrm{d}s,$$

$$[\bar{D}]_{3\times 3} = \int_{\Sigma s}\begin{bmatrix} 1 & 0 & -y \\ 0 & 1 & x \\ -y & x & x^2+y^2 \end{bmatrix}t\,\mathrm{d}s = \begin{bmatrix} A & 0 & 0 \\ 0 & A & 0 \\ 0 & 0 & I_x + I_y \end{bmatrix},$$

where A is the area of cross-section of the thin-walled member; and I_x and I_y are the second moments of inertia of the cross-section with respect to the principal axes x and y respectively.

From Hamilton's principle, taking the first variation of the functional with respect to $\{w\}$ and $\{v_c\}$ in equation (1), and using some standard techniques such as integration by

parts in the derivation, we have the following differential equations and boundary conditions:

$$E[A]_{n\times n}\{w''\} - G[B]_{n\times n}\{w\}_{n\times 1} - G[C]_{n\times 3}\{v_c'\}_{3\times 1} + \rho_0 w^2[A]_{n\times n}\{w\}_{n\times 1} = \{0\}_{n\times 1}, \quad (18)$$

$$G[C]^{\mathrm{T}}_{3\times n}\{w'\}_{n\times 1} + G[D]_{3\times 3}\{v_c''\}_{3\times 1} + \rho_0\omega^2[\bar{D}]_{3\times 3}\{v_c\}_{3\times 1} = \{0\}_{3\times 1}; \quad (19)$$

on the boundaries

$$E[A]_{n\times n}\{w'\}_{n\times 1} = \{0\}_{n\times 1}, \quad (20)$$

$$[C]^{\mathrm{T}}_{3\times n}\{w\}_{n\times 1} + [D]_{3\times 3}\{v_c'\}_{3\times 1} = \{0\}_{3\times 1}; \quad (21)$$

in which the double prime superscript ($''$) represents $\mathrm{d}^2()/\mathrm{d}z^2$, and

$$[D]_{3\times 3} = [D_t]_{3\times 3} + J_d\begin{bmatrix} 0 & & \\ & 0 & \\ & & 1 \end{bmatrix}.$$

Equations (18) and (19) are the governing differential equations for the dynamic analysis of a thin-walled member.

5. SOLUTION OF THE DYNAMIC EQUATIONS

The main differences between the present method and the finite element method can be grouped under two aspects. (1) From the "rigid cross-section" assumption, the lateral displacements at one end of the member element are only three, and the number of longitudinal displacements are n, where n is the number of nodes artificially chosen by which the cross-section is divided in suitable sub-intervals to meet accuracy requirements of analysis for different complexities of the cross-section. The degree of freedom in a member element is then equal to $2n + 6$, and n is not fixed, but depends on the complexity of the cross-section. (2) In the present method, only the longitudinal warping displacements along the cross-section need be interpolated; their distribution along the longitudinal direction can be obtained analytically and will be discussed in this section. Instead of the ordinary interpolation function used in the finite element method, a special interpolation function called the "transformed spline function" described in the previous section, is used in the present method. In matrix form, the end displacements of the member element are expressed by a vector $\{W_E\}$ as

$$\{W_E\}_{(2n+6)\times 1} = [v_{1x}, v_{1y}, \theta_1, w_{11}, w_{12}, \ldots, w_{1n}, v_{2x}, v_{2y}, \theta_2, w_{21}, w_{22}, \ldots, w_{2n}]^{\mathrm{T}}, \quad (22)$$

in which the first subscript 1 or 2 denotes the first ($z = 0$) or second ($z = H$) end cross-section; v_{1x} denotes the lateral displacement of the cross-section in the x direction at the first end; w_{11} denotes the longitudinal displacement of the first node at the first end, etc. Note that n is an arbitrary chosen number of nodes by which the cross-section is divided into sub-intervals to fulfil the accuracy requirements of analysis for different shapes of cross-sections. By this means, the versatility of the method is increased.

Equations (18) and (19) can be written as a standard eigenvalue problem of finite element dynamic equation form, as

$$([K] + \omega^2[M])_{(2n+6)\times(2n+6)}\{W_E\}_{(2n+6)\times 1} = \{0\}_{(2n+1)\times 1}, \quad (23)$$

in which $[M]$ is referred to as the non-linear general mass matrix and can be derived from possible kinetic energy T; $[K]$ is the linear strain stiffness matrix.

From reference [13], the displacement vectors of the member element can be found in terms of the end displacements of the member element:

$$\begin{Bmatrix} v_c \\ w \end{Bmatrix}_{\{n+3\}\times 1} = [N]_{\{n+3\}\times\{2n+6\}} \{W_E\}_{\{2n+6\}\times 1}, \tag{24}$$

in which

$$[N]_{\{n+3\}\times\{2n+6\}} = \begin{pmatrix} [T_v(z)]_{3\times\{2n+6\}} \\ [a]_{n\times n}[T_w(z)]_{n\times\{2n+6\}} \end{pmatrix} [T_E]^{-1}_{\{2n+6\}\times\{2n+6\}}$$

where $[N]$ is a matrix of the interpolation functions,

$$[a]_{n\times n} = [\{a_1\}, \{a_2\}, \ldots \{a_n\}]$$

in which $\{a_i\}$ is an eigenvector;

$$[T_v(z)]_{3\times\{2n+6\}} = \Bigg[-[D]^{-1}_{3\times 3}[C]^{\mathrm{T}}_{3\times n}[a]_{n\times n}\int_0^z [R_0]_{n\times n}\,\mathrm{d}z[a]^{\mathrm{T}}_{n\times n}[C]_{n\times 3} + z\frac{G}{E}[I]_{3\times 3}, [I]_{3\times 3},$$

$$-[D]^{-1}_{3\times 3}[C]^{\mathrm{T}}_{3\times n}[a]_{n\times n}\int_0^z [R]_{n\times 2n}\,\mathrm{d}z\Bigg],$$

$$[T_w(z)]_{n\times\{2n+6\}} = [[R_0]_{n\times n}[a]^{\mathrm{T}}_{n\times n}[C]_{n\times 3}, [0]_{n\times 3}, [R]_{n\times 2n}],$$

$$[T_E]_{\{2n+6\}\times\{2n+6\}} = \begin{bmatrix} [T_v(0)_{3\times\{2n+6\}} \\ [a]_{n\times n}[T_w(0)]_{n\times\{2n+6\}} \\ [T_v(H)]_{3\times\{2n+6\}} \\ [a]_{n\times n}[T_w(H)]_{n\times\{2n+6\}} \end{bmatrix},$$

$$[R_0]_{n\times n} = \begin{bmatrix} \frac{z^2}{2} & & & & & & \\ & \frac{z^2}{2} & & & 0 & & \\ & & \frac{z^2}{2} & & & & \\ & & & -\frac{1}{\Lambda_4}\frac{E}{G} & & & \\ & 0 & & & \ddots & & \\ & & & & & -\frac{1}{\Lambda_n}\frac{E}{G} \end{bmatrix},$$

$$[R]_{n\times 2n}=\begin{bmatrix} z,1 & & & & & & & \\ & z,1 & & & & 0 & & \\ & & z,1 & & & & & \\ & & & \mathrm{e}^{-\lambda_4\xi},\,\mathrm{e}^{-\lambda_4\eta} & & & & \\ & & & & \cdot\cdot & & & \\ & & & & & \cdot\cdot & & \\ & & 0 & & & & \cdot\cdot & \\ & & & & & & & \mathrm{e}^{-\lambda_n\xi},\,\mathrm{e}^{-\lambda_n\eta} \end{bmatrix},$$

$$\eta=\frac{z}{H},\qquad \xi=1-\eta,\qquad \lambda_i=H\sqrt{\frac{G}{E}\Lambda_i},$$

where $\Lambda_1, \Lambda_2, \ldots, \Lambda_n$ are the eigenvalues of the eigenvalue equation.

Following the standard procedures of the finite element method, the spline member element's stiffness matrix $[K]$ can be obtained.

Substituting equation (24) into equation (17) yields

$$T=\tfrac{1}{2}\omega^2\{W_E\}^{\mathrm{T}}_{1\times\{2n+6\}}[M]_{\{2n+6\}\times\{2n+6\}}\{W_E\}_{\{2n+6\}\times 1}, \tag{25}$$

in which

$$[M]_{\{2n+6\}\times\{2n+6\}}=([T_E]^{-1})^{\mathrm{T}}_{\{2n+6\}\times\{2n+6\}}\int_0^H \rho_0([T_v(z)]^{\mathrm{T}}_{\{2n+6\}\times 3}[\bar{D}]_{3\times 3}[T_v(z)]_{3\times\{2n+6\}} + [T_w]^{\mathrm{T}}_{\{2n+6\}\times n}[a]^{\mathrm{T}}_{n\times n}[a]_{n\times n}[T_w]_{n\times\{2n+6\}})\,\mathrm{d}z[T_E]^{-1}_{\{2n+6\}\times\{2n+6\}}. \tag{26}$$

6. NUMERICAL EXAMPLES

Cantilever thin-walled members with four shapes of cross-sections, as shown in Figure 4, are studied by the proposed method for vibration analysis. In the presentation of the results, the characteristics of the mode shapes are simply described by labels, in which BX and BY denote the bending mode in the x and y directions respectively, while BA denotes the axial vibration in the z direction and BT denotes the torsion mode around the z-axis.

Example 1. The thin-walled member with a channel-shaped cross-section as shown in Figure 4(a) is discussed for vibration analysis. The related data are as follows: $E=3{\cdot}0\times10^6\ \mathrm{KN/m^2}$; the Poisson ratio, $v=0{\cdot}15$; $t=0{\cdot}2$ m; $\rho_0=2500\ \mathrm{kg/m^3}$; the total height of the member $H_t=15{\cdot}0$ m. In the example, the numerical solution in the present paper is compared with the available solution by the "COSMOS/M" finite element analysis program [15] and another analytical method [14] for the same member, as shown in Table 1. Comparing the present results with those of Capuani ones, good agreement can be seen for the thin-walled members except for the sixth frequency. From the table it can be observed that the results obtained by the present method and COSMOS/M have some differences, but they are all under 8·0%. In addition, the spline finite member element method has several advantages over the COSMOS finite element analysis program when applied to thin-walled structures. These include the greatly reduced number of degrees of freedom for the given structural system amounting to only 680 degrees of freedom. In the same example, a considerably larger number of degrees of freedom is required in the finite element analysis compared with the present method. The total system data of the COSMOS program are as follows: number of equations = 1860; number of matrix

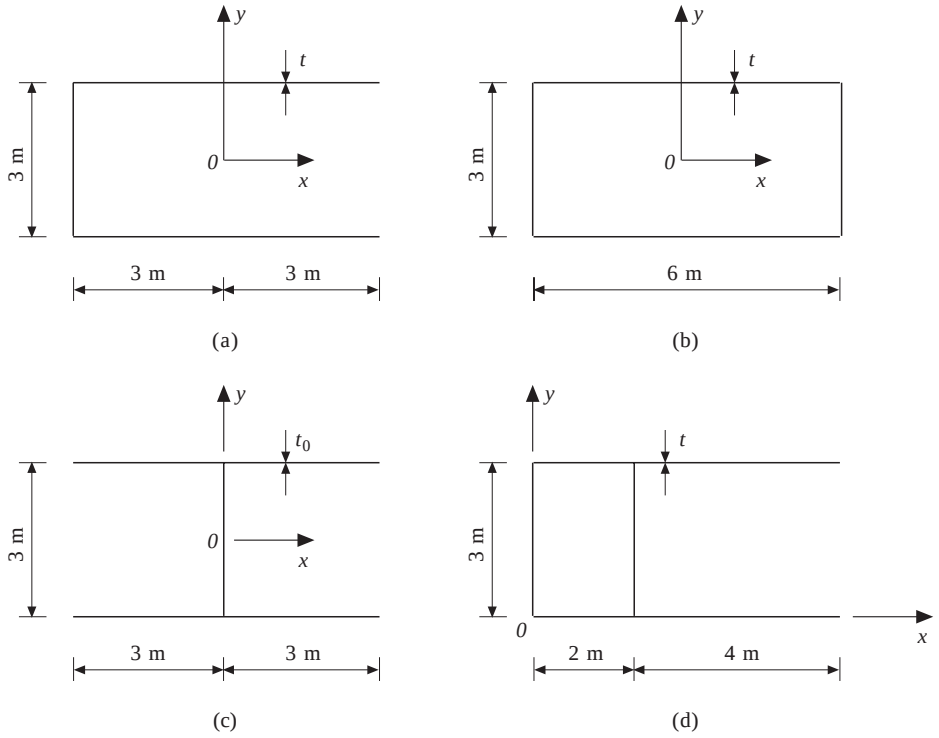

Figure 4. The cross-section of the thin-walled members.

elements = 521 714; mean half-bandwidth = 1803; number of elements = 900; number of nodal points = 341, resulting in a heavy consumption of CPU time and data preparation and manipulation efforts.

Example 2. The thin-walled member with a rectangle-shaped cross-section shown in Figure 4(b) is analyzed for the dynamic analysis. The useful data are as follows: $E = 3{\cdot}0 \times 10^6\ \mathrm{KN/m^2}$; $E/G = 2{\cdot}3$; $t = 0{\cdot}4$ m; $\rho_0 = 2500\ \mathrm{kg/m^3}$; $H_t = 15$ m. This example has been investigated in reference [16]. The first eight natural frequencies are compared with the method mentioned above and the available solution by the "COSMOS/M" finite element analysis program [15] in Table 2.

The comparison of the results in Table 2 shows that the proposed method is efficient and accurate for thin-walled closed members.

TABLE 1

Comparisons of the results of Example 1

Mode no.	Capuani *et al*. [14]	COSMOS [15] mesh, 30 × 10	Present method	Mode shape
1	22·9	25·9611	24·0518	BY
2	—	92·8102	97·9921	BX, BA
3	110·3	121·2504	113·8121	BY
4	125·4	128·5741	132·9215	BY, BA, BT
5	247·0	277·0317	247·5250	BY
6	364·8	364·6105	354·5467	BY
7	392·9	366·5328	400·6028	BY

TABLE 2

Comparisons of the results of Example 2

Mode no.	Laudiero *et al*. [16]	COSMOS [15] mesh, 36 × 10	Present method	Mode shape
1	61·10	61·7288	63·8695	BY
2	—	100·7278	106·2159	BX, BA
3	189·0	188·2396	187·2816	BT
4	244·1	245·1885	252·1227	BY
5	—	406·2652	401·6215	BX, BA
6	515·6	513·9982	521·9535	BY
7	568·9	561·9905	564·5677	BT
8	760·3	752·3274	786·8634	BY

TABLE 3

Comparisons of the results of Example 3

Mode no.	Capuani *et al*. [14]	ODE solver [17]	Present method	Mode shape
1	57·7	57·99	60·7692	BT
2	—	59·34	61·9695	BY
3	—	76·11	80·8645	BX, BA
4	—	214·1	221·7987	BY
5	250·7	251·3	263·8864	BT, BA
6	—	362·8	361·0387	BX, BA
7	—	435·0	443·8796	BY
8	540·5	545·0	556·6316	BY, BA

Example 3. An open I-shaped cross-section as shown in Figure 4(c), which was originally Capuani's example [14], is studied for vibration analysis. The first eight circular frequencies from various methods are tabulated in Table 3. The data are as follows: $E = 3{\cdot}0 \times 10^6\ \mathrm{KN/m^2}$; $E/G = 2{\cdot}3$; $t = 0{\cdot}2\ \mathrm{m}$; $\rho_0 = 2500\ \mathrm{kg/m^3}$; $H_t = 15\ \mathrm{m}$.

From Table 3 it can be seen that the results given by the proposed method and ODE solver are close to each other.

Example 4. A cross-section composed of a rectangular box section with two outstanding flanges, as shown in Figure 4(d), is investigated for vibration analysis. The data are as follows: $E = 3{\cdot}0 \times 10^6\ \mathrm{KN/m^2}$; $E/G = 2{\cdot}3$; $t = 0{\cdot}2\ \mathrm{m}$; $\rho_0 = 2500\ \mathrm{kg/m^3}$; $H_t = 15\ \mathrm{m}$. The numerical solution in the present paper is compared with the available solution by using ODE solver [17] and another analytical method [14] for the same member, as shown in Table 4.

TABLE 4

Comparisons of the results of Example 4

Mode no.	Capuani *et al*. [14]	ODE solver [17]	Present method	Mode shape
1	47·3	51·76	53·9611	BY, BT
2	—	84·52	89·6907	BX
3	130·4	127·4	131·6682	BY, BT
4	170·8	203·5	208·9655	BY, BT
5	294·0	338·1	365·9100	BX, BA
6	—	362·8	393·4237	BY, BT
7	421·7	421·6	448·7700	BY, BA, BT
8	—	607·9	610·2427	BY, BT

TABLE 5

Effect of number of section nodes, n, on the natural frequency

Mode no.	$n = 9$	$n = 14$	$n = 15$
1	24·052496	24·051927	24·051849
2	97·994656	97·992214	97·992123
3	113·910684	113·873514	113·873514
4	132·927734	132·920993	132·921512
5	249·808318	248·965643	247·525003
6	366·885542	362·551934	354·546709
7	400·661146	400·605999	400·602763

From Table 4 it can be seen that the results given by the proposed method and ODE solver are close to each other. Compared with Capuani's method, some greater differences can be observed.

7. CONVERGENCE STUDIES

An important part of an eigenvalue and vector solution is to estimate the accuracy with which the required eigensystem has been calculated. The solution is terminated once convergence within the prescribed tolerances has been obtained. Because the transformed B_3-spline function is taken as the interpolation function of longitudinal displacement of the cross-section, example 1 in the present paper is used to investigate the rate of convergence of the natural frequency of the thin-walled members using the proposed method with increasing numbers of section nodes, as shown in Table 5.

It can be seen from the above table that the numerical results can converge very rapidly to stable results. The convergence of the results fully demonstrates the efficiency of the transformed B_3-spline function. In Table 6 is shown the effect of the number of member elements along the longitudinal direction on the natural frequencies in which the data come from example 4. Table 6 demonstrates the convergence of the solution for the cantilever thin-walled member. From the convergence study in that section of the paper, the accuracy of the solution is determined not only by the number of segment of the cross section and of its sub-intervals, but also by the number of member elements into which a member is divided along the longitudinal direction.

TABLE 6

Effect of number of member elements, e, on natural frequencies

Mode no.	$e = 18$	$e = 19$	$e = 20$
1	54·166589	54·058419	53·961078
2	90·069106	89·869749	89·690674
3	131·901823	131·778134	131·668236
4	209·124943	209·044644	208·965535
5	366·107382	366·015002	365·909990
6	394·072896	393·771889	393·423697
7	448·781120	448·778784	448·781120
8	611·875245	611·117729	610·242744

8. CONCLUSIONS

Based on the energy method, a systematic method, called the spline finite member element method, is developed for dynamic analysis of thin-walled members with arbitrary cross-section in the present paper. According to the above discussions, the following conclusions can be drawn:

(a) The proposed method has an advantage over methods based on the classical theory [1] because the effect of the shearing strains of the middle surface of walls, which reflect the shear lag phenomenon, on the vibration is considered.

(b) The transformed B_3-spline function is used to simulate the warping displacement along the cross-section of the thin-walled member. By using the spline function as an interpolation function, a cross-section will be divided into equal or unequal segments to meet some special need. This arrangement greatly improves the flexibility of the transformed spline function. Because the parameters of the transformed spline function in every segment are the real node displacement parameters, this overcomes the difficulty of the ordinary spline function in simulating the longitudinal displacements of cross section with branches of walls.

(c) Because there is no need to introduce the concepts of shear center and sectorial co-ordinate, this method is easily understood and applied. It can be used to analyze the closed cross-section member as conveniently as the open cross-section without extra labor.

(d) Compared with the results from the "COSMOS/M" finite element analysis program and other analytical methods, the numerical examples proposed in this paper demonstrate the versatility, accuracy and efficiency of the proposed method.

(e) The convergence shown in the above numerical examples predicts the reliability of the results.

REFERENCES

1. V. P. Vlasov 1961 *Thin-walled Elastic Beams*. Israel, Jerusalem: Israel Program for Scientific Translations; second edition.
2. A. C. Heidebrecht and K. R. Ravindora 1971 *Journal of Engineering Mechanics*, *American Society of Civil Engineers* **97**, 239–252. Frequency analysis of thin-walled shear walls.
3. T. M. Roberts 1987 *Journal of Engineering Mechanics*, *American Society of Civil Engineers* **113**, 1584–1593. Free vibrations of thin-walled bars.
4. W. Weaver and P. R. Johnston 1987 *Structural Dynamics by Finite Elements*. Englewood Cliffs, New Jersey: Prentice-Hall.
5. S. P. Timoshenko, D. H. Young and W. Weaver 1974 *Vibration Problems in Engineering*. New York: John Wiley; fourth edition.
6. G. R. Cowper 1966 *Journal of Applied Mechanics* **33**, 335–339. The shear coefficient in Timoshenko's beam theory.
7. G. R. Cowper 1968 *Journal of Engineering Mechanics*, *American Society of Civil Engineers* **94**, 1447–1453. On the accuracy of Timoshenko's beam theory.
8. P. O. Friberg 1985 *International Journal of Numerical and Mechanical Engineering* **21**, 1205. Beam element matrices derived from Vlasov's theory of open thin-walled elastic beams.
9. S. Gellin and G. C. Lee 1988 *Finite Element Analysis of Thin-Walled Structures*. *Finite element available for the analysis of non-curved thin-walled structures* 1–30. London and New York: Elsevier Applied Science.
10. D. Krajcinovic 1969 *International Journal of Solids and Structures* **5**, 639–662. A consisted discrete element technique for thin-walled assemblages.
11. Q.-F. Wang and W. Y. Li 1996 *Computational Mechanics* **18**, 139–146. Buckling of thin-walled compressive with shear lag using spline finite member element method.
12. W. C. Bruce, O. G. Keith *et al*. 1991 *Maple Language Reference Manual*. Waterloo: Waterloo Maple.
13. Q.-F. Wang and W. Y. Li 1996 *J. Comp. Meths. Appl. Mech. Engng*. **136**, 259–271. Spline finite

member element method for buckling of thin-walled members with any cross sections in pure bending.
14. D. Capuani, M. Savoid and F. Laudiero 1992 *International Journal of Earthquake Engineering and Structural Dynamics* **21**, 859–879. A generalization of the Timoshenko beam model for coupled vibration analysis of thin-walled beams.
15. M. Lashkari 1988 *COSMOS/M User's Guide*. California: Structural Research and Analysis Corporation.
16. F. Laudiero and M. Savoid 1991 *Journal of Thin-walled Structures* **11**, 375–407. The shear strain influence on the dynamics of thin-walled beams.
17. K. Xin 1995 *Ph.D. Thesis*, *The Hong Kong Polytechnic University*. A semi-discrete method using transformed spline function for thin-walled structures with shear effect.